SCIENCE CHINA
Chemistry

• ARTICLES •

September 2014 Vol.57 No.9: 1291–1299
doi: 10.1007/s11426-014-5119-6

Simultaneous removal of uranium and humic acid by cyclodextrin modified graphene oxide nanosheets

SONG WenCheng[1,2], SHAO DaDong[2], LU SongSheng[3] & WANG XiangKe[1,2*]

[1]*School of Nuclear Science and Technology, University of Science and Technology of China, Hefei 230026, China*
[2]*Institute of Plasma Physics, Chinese Academy of Sciences, Hefei 230031, China*
[3]*New Star Institute of Applied Technology, Hefei 230031, China*

Received November 27, 2013; accepted January 21, 2014; published online July 31, 2014

Cyclodextrin-modified graphene oxide nanosheets (denoted as CD/GO) were synthesized by an *in-situ* polymerization method and characterized by as well as Fourier transform-infrared spectroscopy, X-ray photoelectron spectroscopy, Raman spectroscopy and potentiometric acid-base titration. The characterization results indicated that CD was successfully grafted onto GO surfaces by forming a chemical bond. Mutual effects on the simultaneous removal of hexavalent uranium and humic acid by CD/GO from aqueous solution were investigated. The results indicated that U(VI) and humic acid (HA) sorption on CD/GO were greatly affected by pH and ionic strength. The presence of HA enhanced U(VI) sorption at low pH and reduced U(VI) sorption at high pH, whereas the presence of U(VI) enhanced HA sorption. The surface adsorbed HA acted as a "bridge" between U(VI) and CD/GO, and formed strong inner-sphere surface complexes with U(VI). Sorption isotherms of U(VI) or HA on CD/GO could be well fitted by the Langmuir model. This work highlights that CD/GO can be used as a promising material in the enrichment of U(VI) and HA from wastewater in U(VI) and humic substances obtained by environmental pollution cleanup.

graphene oxide, uranium, humic acid, cyclodextrin, simultaneous sorption

1 Introduction

The large specific surface area of graphene (about 2620 m^2/g) [1, 2], ensures its potential for applications in environmental pollution control and remediation [3–5]. Graphene oxide (GO), one of the important graphene derivatives, has plenty of oxygen atoms on the basal plane and at the edges of the sheets in the form of epoxy, hydroxyl, and carboxyl groups [6]. These oxygen-containing groups can bind metal ions [7] and organic pollutants [8, 9] through coordination, electrostatic interaction, hydrogen bonding. However, GO has a tendency to aggregate into layer-by-layer form because of strong interplanar interactions. As a result, however, a considerable part of the surface areas of the layers will be lost [10, 11]. Therefore, it is necessary to modify the surface of GO to solve these problems. Cyclodextrins (CDs) are cyclic oligosaccharides with internal hydrophobic and external hydrophilic cavities [12, 13]. One type of CD, β-CD, has been shown to form strong complexes with organic pollutants and metal ions [14–16], which means that the modification of CD onto GO surfaces can effectively enhance its sorption capacity. We studied the potential application of β-CD-modified GO (CD/GO) as a possible broad-spectrum sorbent for water purification.

The release of radionuclides into the environment has caused research to be focused on the development of accurate and adaptable tools to remove these contaminants [17, 18]. Uranium, in particular, is a highly poisonous toxin that has a tremendous and long-lasting impact on the environment. Disposed into water, uranium can ultimately go into

*Corresponding author (email: xkwang@ipp.ac.cn)

the food chain and be adsorbed by human, which causes human organ damage [19] and even cancer. For the sake of human health, the development of materials and techniques for the effective preconcentration of uranium from aqueous solution has become an urgent issue.

Humic acid (HA) is widely present in soils, sediments, and natural waters. It has lots of organic functional groups [20] that provide abundant binding sites for heavy-metal ions. HA can also influence heavy-metal ion dispersion and mobility in the environment [20]. The elimination of HA from aqueous solution is therefore of great practical significance [21].

In this study, CD/GO was synthesized by *in-situ* polymerization techniques and characterized by SEM, FT-IR spectroscopy, XPS spectroscopy, Raman spectroscopy, and potentiometric acid-base titrations. Using a batch-sorption technique, the simultaneous and single sorption of CD/GO toward U(VI) and/or HA from aqueous solutions were assessed.

2 Experimental

2.1 Materials

GO was synthesized from graphite with the reformative Hummers method [22, 23]. Briefly, under mechanical stirring and an ice water bath environment, 1.5 g of graphite, 1.5 g of sodium nitrate, and 60 mL of sulfuric acid were mixed in an Erlenmeyer flask. Afterward, 9.0 g of potassium permanganate was lightly added, and then the mixture was reacted at 20 ± 1 °C for 5 d. After 120 mL water was added, the mixture was churned for 40 min at 90 °C, and then cooled to 60 °C. The 6 mL peroxide (30%) was added slowly to remove possible residual potassium permanganate. After the solution was filtered, the filter residue was washed thoroughly and dried under vacuum.

The CD/GO was prepared by GO (0.01 g) in 200 mL solution containing 3.6 g CD next, the pH was adjusted to 11 by the addition of ammonia solution [24]. Using a water bath at 60 °C, 2.0 mL hydrazine solution was added to initiate the modification reaction. After reaction for 5 h, the solution was filtered. The filter residue was washed thoroughly and then dried at 60 °C for 24 h.

2.2 Characterization

The synthesized CD/GO and GO were characterized by scanning electron microscopy (SEM), Fourier transform infrared spectroscopy (FT-IR), X-ray photoelectron spectroscopy (XPS), Raman spectroscopy, and potentiometric acid-base titrations. SEM images were obtained on a field-emission scanning electron microscope (FEI-JSM 6320F, JEOL, Japan). FT-IR spectroscopy was carried out on a Perkins Elmer 100 spectrometer (Perkin-Elmer, America) in a KBr pellet. The XPS spectrum was taken using an ESCALAB 250 system (VG Scientific, America) with a multi-detection analyzer using a monochromatized Al-Kα source under a 10^{-8} Pa residual pressure. The Raman spectrum was carried out on a LabRam HR Raman spectrometer (Horiba Jobin Yvon, France) at an excitation of 514.5 nm by Ar^{+} laser. Potentiometric acid-base titrations were conducted using a computer-controlled titration system (DL50 Automatic Titrator, Mettler Toledo, Switzerland).

2.3 Sorption experiments

Sorption of U(VI) and/or HA on GO or CD/GO were carried out with a batch-sorption technique. The sorbent was mixed with $NaClO_4$, HA, and U(VI) in polyethylene test tubes, based on the required concentration of the various constituents. The suspension was regulated to required pH values by adding trace amounts of 0.1 or 0.01 mol/L perchloric acid or sodium hydroxide, and then was shaken for 24 h to achieve full sorption equilibrium. The polyethylene test tubes were centrifuged at 18000 rpm for 20 min to separate the sorbent from the liquid phases. The concentration of HA was analyzed by UV-Vis spectrophotometer (Shimadzu, Japan) at 259.6 nm, and the U(VI) concentration was determined by the Arsenazo III spectrophotometric method at the wavelength of 650 nm. The adsorbed amounts of U(VI) or HA on CD/GO or GO were calculated from the difference between the initial and final concentrations. The sorption percentage and the distribution coefficient (K_d) were calculated from the following equations:

$$\text{Sorption}\,\% = \frac{C_0 - C_e}{C_0} \times 100\% \quad (1)$$

$$K_d = \frac{C_0 - C_e}{C_e} \times \frac{V}{m} \quad (2)$$

where C_0 (mg/L) is the initial concentration, C_e (mg/L) is the final concentration, m (g) is the mass of CD/GO or GO, and V (L) is the volume of suspension.

The mutual effects of HA and U(VI) with CD/GO were also researched. Batch tests were as follows: CD/GO, $NaClO_4$, and U(VI) were equilibrated for 24 h before the addition of HA (Batch A); HA, $NaClO_4$, and CD/GO were equilibrated for 24 h before the addition of U(VI) (Batch B); and HA, U(VI), and $NaClO_4$ were equilibrated for 24 h before the addition of CD/GO (Batch C).

3 Results and discussion

3.1 Characterization of CD/GO

SEM images of GO and CD/GO are shown in Figures 1(a) and (b). The differences of the surface morphology between GO and CD/GO are distinctly observed. As can be seen

from Figure 1(a), the surface of GO is smooth and there are few wrinkles, whereas Figure 1(b) depicts a more wrinkled surface of CD/GO with attached nanoparticles, which indicates the formation of CD on GO surfaces.

Figure 1(c) illustrates the FT-IR spectra of CD, CD/GO, and GO. In the spectrum of GO, the peak at ~3400 cm^{-1} is due to the O–H stretching vibration of hydroxyl groups on sorbent surfaces. A C–O group at ~1220 cm^{-1} and ~1100 cm^{-1}, a C=O group at ~1730 cm^{-1}, and a C=C group at ~1620 cm^{-1} can be detected. In the spectrum of CD, the peak at ~2924 cm^{-1} corresponds to the C–H-stretching vibration. A coupled C–C/C–O group at ~1159 cm^{-1} and an anti-symmetric glycosidic bond C–O–C group at ~1032 cm^{-1} are also found [25]. As for CD/GO, the characteristic peaks mentioned above are clearly detected, which proves successful modification of CD onto GO surfaces.

The oxygen-containing functional groups on the surfaces of GO and CD/GO composite were investigated by XPS. The O 1s XPS spectra of GO and CD/GO show three peaks, at 531.4 ± 0.2, 532.7 ± 0.2, and 533.7 ± 0.2 eV, which correspond to –COOH, >C=O and –C–OH bonds, respectively. As seen in Figure 1(d), after the GO is grafted with CD, the peak fractions of –COOH and >C=O reduce and the peak fraction of –C–OH increases. Quantitative analyses of the O 1s spectra of GO and CD/GO are shown in Table 1. Due to the fact that CD contains large amounts of hydroxyl groups [26], the modified CD on GO distinctly increases the peak fraction of –C–OH.

Raman spectra of GO and CD/GO demonstrated two main bands, the G peak at ~1581 cm^{-1} and the D peak at ~1351 cm^{-1}. I_G/I_D can assess the degree of structural defects. Raman spectra (Figure 1(e)) analysis indicates that the I_G/I_D

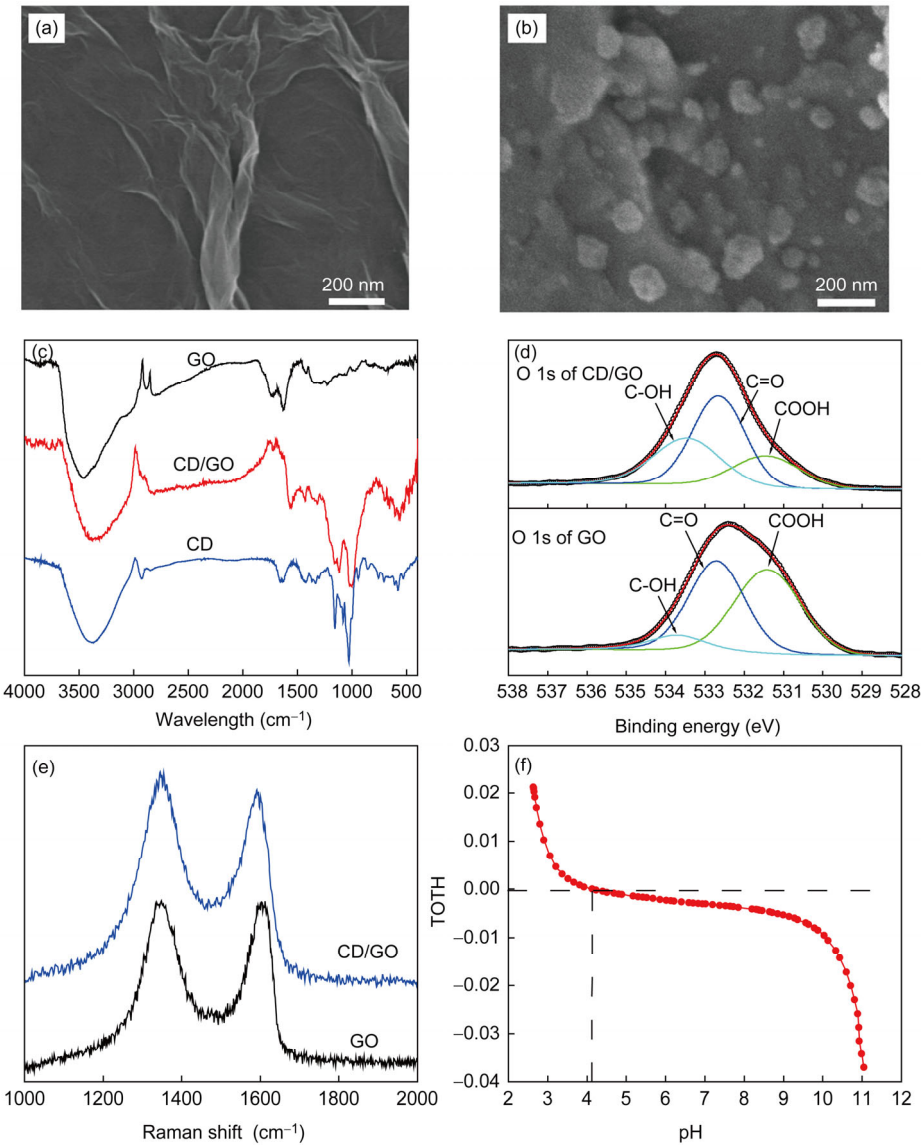

Figure 1 (a) SEM image of GO, (b) SEM image of CD/GO, (c) FT-IR spectra of GO, CD and CD/GO, (d) XPS spectra of GO and CD/GO, (e) Raman spectra of GO and CD/GO, (f) potentiometric acid-base titration of CD/GO. TOTH is the total concentration of consumed protons.

Table 1 Curve fitting results of XPS O 1s spectra

	Peak	BE[a] (eV)	FWHM[b] (eV)	Fraction (%)
GO	–COOH	531.40	1.98	46.7
	>C=O	532.70	1.67	44.9
	–C–OH	533.70	1.67	8.38
β–CD/GO	–COOH	531.44	2.02	35.8
	>C=O	532.65	1.58	28.2
	–C–OH	533.66	2.03	36.0

a) Binding energy; b) full width at half-maximum.

value of GO markedly decreases from 0.93 to 0.87 after CD grafting, which indicates that CD is successfully modified onto the GO surface.

The potentiometric acid-base titration of CD/GO is shown in Figure 1(f). Assuming that surface sites of CD/GO (SOH) are amphoteric, they are positively charged at low pH because of the protonation reaction (i.e., $SOH + H^+ \rightleftharpoons SOH_2^+$), and are negatively charged at high pH because of the deprotonation reaction (i.e., $SOH \rightleftharpoons SO^- + H^+$). The titration curve was collected in 0.01 mol/L $NaClO_4$ solution from pH 2.0 to pH 11.0 (adjusted by $HClO_4$ or NaOH). As seen in Figure 1(f), the point of zero change (pH_{pzc}) of CD/GO is about 4.13. Obviously, the trend of surface charge tremendously affects the sorption capacity of CD/GO to U(VI) and HA at different pH values.

3.2 Effect of initial pH

Single and simultaneous sorption of U(VI) and/or HA on CD/GO are greatly influenced by the initial pH (Figure 2). In the case of single U(VI) sorption (i.e., in the absence of HA) on CD/GO, the sorption increases from about 5% to 80% when the pH value increases from 2.0 to 6.0, and then rapidly reduces at pH > 6.0. Both distribution of U(VI) species and the surface charges of CD/GO can be affected by changing the initial pH values. Protonation-deprotonation reactions of functional groups can promote or suppress the sorption of metal ions. From the potentiometric acid-base titration (Figure 1(f)), one can see that the surface of CD/GO is positively charged at pH < 4.13. Meanwhile, the dominant U(VI) species is UO_2^{2+} [25], and the electrostatic repulsion between CD/GO and UO_2^{2+} lowers the sorption ability. As pH value increases, the surface of CD/GO gradually becomes negatively charged. Moreover, functional groups of CD/GO surface become more decentralized. The two variation trends mentioned above increase the sorption ability between CD/GO and $(UO_2)_3(OH)_5^+/(UO_2)(OH)^+$, which are the dominant species of U(VI) at pH 4.0 ~ 6.0. When the pH of the aqueous solution is more than 7.0, the surface charge of sorbent becomes more negative and the main species of U(VI) are $(UO_2)_3(OH)_7^-/UO_2(OH)_3^-$. The repulsion between $(UO_2)_3(OH)_7^-/UO_2(OH)_3^-$ and surface charges results in the drop of sorption. Similar results were also reported for UO_2^{2+} sorption to tea waste [27] and on plasma-functionalized carbon nanotubes [28]. However, simultaneous sorption of U(VI) (i.e., in the presence of HA) shows a drastically different trend compared to single sorption of U(VI). When pH is < 6.0, the sorption percentage of U(VI) on CD/GO is improved and the maximum sorption is about 10% higher than that of U(VI) on CD/GO in the absence of HA. However, when pH > 6.0, the presence of HA reduces U(VI) sorption. HA remains negatively charged due to its $pH_{pzc} \approx 2$ [29]. When pH is low, the electrostatic interaction makes HA sorption on CD/GO easy, and then forms strong complexes with U(VI), which results in improving U(VI) sorption onto CD/GO. When pH is high, more HA molecules remain in solution and the strong complexation of HA with U(VI) is formed, which reduces U(VI) sorption onto CD/GO. In other words, fewer HA molecules are adsorbed onto CD/GO, indicating that fewer U(VI) ions form surface complexes with surface-adsorbed HA on CD/GO surfaces. As pH increases, the sorption of U(VI) reduces accordingly with HA.

Figure 2(a) also demonstrates single sorption of HA (i.e., in the absence of U(VI)) on CD/GO reduces as pH increases.

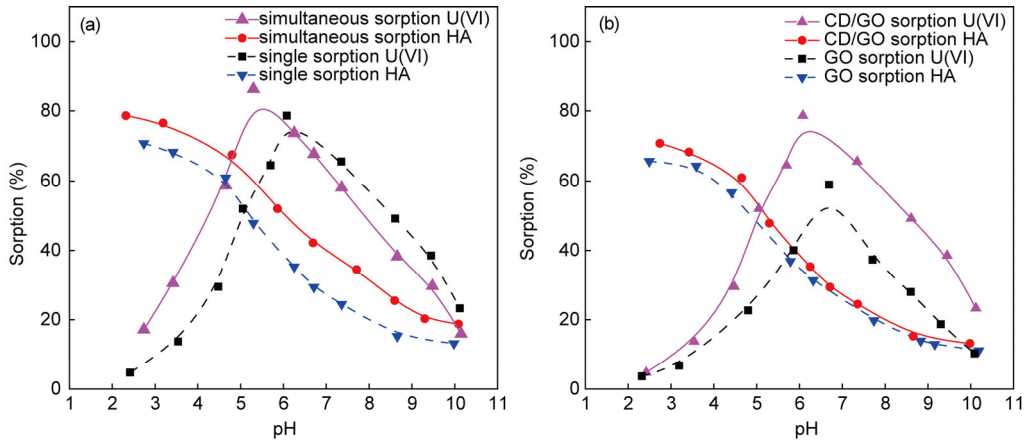

Figure 2 (a) Effect of pH on single and simultaneous sorption of U(VI) and HA on CD/GO and (b) effect of pH on U(VI) and HA sorption to CD/GO and GO. T = 288 K, m/V = 0.1 g/L, I = 0.01 mol/L $NaClO_4$, C[U(VI) $_{(initial)}$] = 24 mg/L, C[$HA_{(initial)}$] = 10 mg/L.

At lower pH, CD/GO is positively charged due to protonation (i.e. SOH + $H^+ \rightleftharpoons SOH_2^+$) while HA is negatively charged, which increases the sorption of HA onto CD/GO because of electrostatic attraction. As pH is increased, both CD/GO and HA become negatively charged. As a result, the sorption of HA onto CD/GO is greatly reduced because of electrostatic repulsion. In addition, when pH is low, HA is strongly compressed duo to low surface charge [30] and the CD/GO sites that are occupied by HA become smaller. Nevertheless, when pH is high, HA is strongly stretched due to electrostatic repulsion within the HA itself. Therefore, a larger surface of CD/GO is occupied by HA molecules (another reason that the sorption percentage of HA onto CD/GO is higher at lower pH and is lower at higher pH). At all pH values, the existence of U(VI) improves HA sorption on CD/GO under experimental conditions (Figure 2(a)). The interactions between HA and U(VI) in solution affect HA species distribution and thereby influences HA sorption. The interactions between HA and U(VI) can alter the spacing and packing of HA and can also neutralize the repulsive forces between CD/GO and HA.

Figure 2(b) indicates that the sorption of U(VI) on GO increases as pH is increased from 2 to 7, and then reduces steeply at pH > 7. The trend of U(VI) sorption on GO is similar to that of U(VI) sorption on CD/GO. The sorption of HA on GO and CD/GO decreases with the increase of pH. However, one can see that the sorptions of U(VI) and HA on CD/GO are higher than those of U(VI) and HA on GO, which demonstrates that the CD-modified GO surfaces can effectively increase the sorption ability of CD/GO. From these results, one can see that the presence of HA can enhance U(VI) sorption at low pH values but reduces U(VI) sorption at high pH values. This effect is attributed to the interaction of HA with CD/GO and the surface properties of HA and CD/GO.

3.3 Effect of ionic strength

Assessment of ionic strength will help validate practical-use ability of sorbents for wastewater treatment. From Figure 3(a), one can see that the sorption of U(VI) on CD/GO decreases as $NaClO_4$ concentration increases. When uranium ions are present in a liquid of high ionic strength, their activity is heavily decreased, which inhibits their move to the surface of CD/GO. Moreover, high ionic strength can decrease the electrostatic repulsion between CD/GO, which results in aggregation and lower adsorption ability of CD/GO. The ionic strength-dependence of uranium sorption indicates a surface complexation mechanism [25].

As shown in Figure 3(b), ionic strength can greatly influence the sorption percentage of HA on CD/GO. As ionic strength increases, HA is further compressed and becomes smaller [31, 32]. This is the reason that more HA molecules can be adsorbed on CD/GO at higher ionic strengths.

3.4 Effect of sorbent content

The sorption of U(VI) is not only dependent on pH values and its relative species at different pH values (Figure 4(a)), but also dependent on solid content. The effect of sorbent content on the sorption of U(VI) and HA is shown in Figure 4(b). The sorption of U(VI) and HA distinctly increases as sorbent content increases, because the functional sites that are involved in the sorption of U(VI) and HA increase as sorbent content increases. The distribution coefficient (K_d) reduces slightly as solid content increases. According to their physicochemical properties, the K_d values are independent of solid contents at low solid-content concentrations. However, it is inevitable that the competition among the solid particles will reduce the effective sites of the functional groups on CD/GO surfaces, which causes the sorption capacity to be decreased with the increase of solid contents. In this manner, K_d values decrease with the increase of solid contents.

3.5 Simultaneous sorption

The enhancement of simultaneous sorption of U(VI) and HA on CD/GO may belong to: (I) electrostatic interaction; (II) the formation of ternary cation-anion surface complex; and (III) the formation of surface precipitate [33]. To differentiate the above mechanisms, we performed three batch tests. As seen in Figure 5(a), the amounts of U(VI) adsorbedby CD/GO for various batch tests reduce in this sequence: Batch A > Batch C > Batch B. The HA concentration (denoted as C_{HA}) significantly affects U(VI) sorption. In addition, the mechanisms of the three batch tests are different. U(VI) sorption increases as C_{HA} increases at C_{HA} < 8 mg/L. These observed differences suggest the differences in the mechanisms of U(VI) sorption on CD/GO. The effect of HA on U(VI) sorption on CD/GO is attributed to the formation of HA-U complexes on CD/GO surfaces that can promote the sorption of U(VI), i.e., the formation of ternary cation-anion surface complexes. As C_{HA} increases, more U(VI) ions are adsorbed on CD/GO, because more functional groups of HA (such as HO– and COO–) are provided to form the HA-U(VI) complexes. However, at C_{HA} > 8 mg/L, redundant HA molecules form complexes with U(VI) which results in the stabilizing U(VI) ions in aqueous solutions. In addition, the aggregation of HA-U(VI) monomers would occur at higher C_{HA} [34]. The latter may be the reason that the sorption of U(VI) does not basically change at 8 mg/L < C_{HA} < 18 mg/L.

The obvious differences among U(VI) sorptions in the ternary systems obtained via the three batch tests indicate different sorption mechanisms. For the Batch A system, when HA was put into the solution of U(VI)-CD/GO, the complexes of HA and surface-adsorbed U(VI) on CD/GO were unlikely to form. Moreover, a small amount of U(VI) ions that are not adsorbed onto the CD/GO can form com-

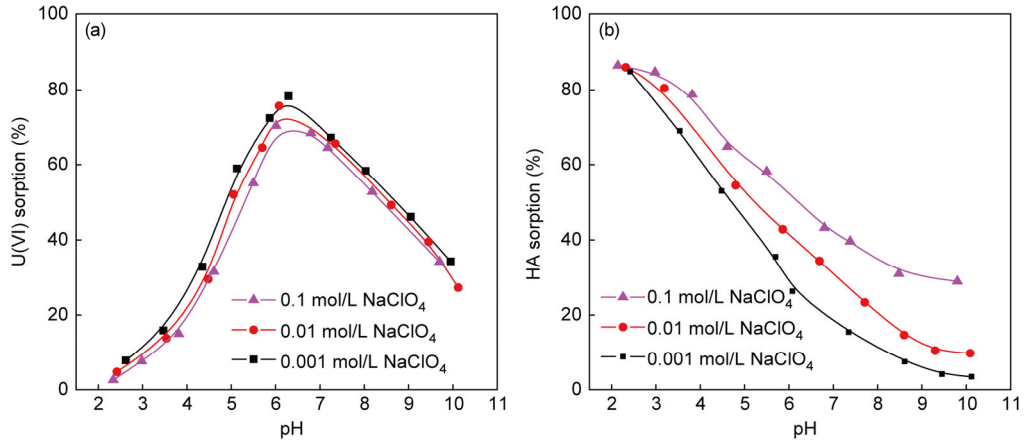

Figure 3 Effect of ionic strength on the sorption of U(VI) (a) and HA (b) onto CD/GO. T = 288 K, m/V = 0.1g/L, C[U(VI) $_{(initial)}$] = 24 mg/L, C[HA$_{(initial)}$] = 10.0 mg/L.

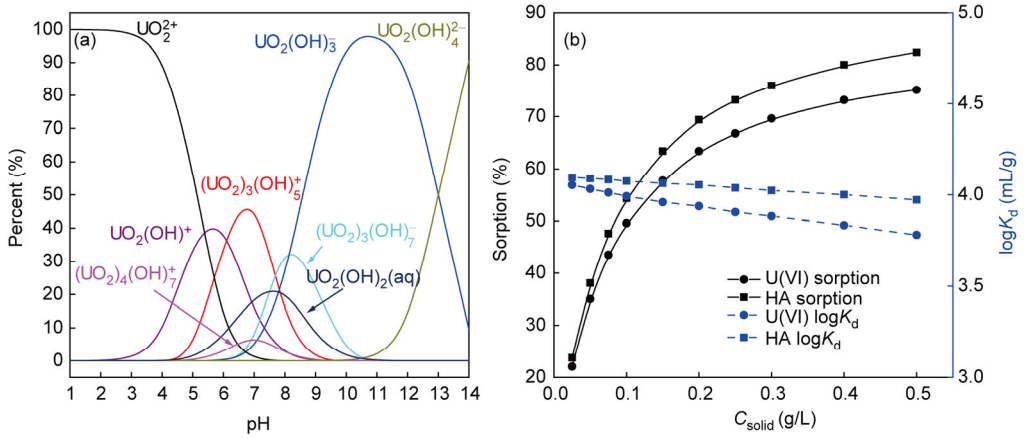

Figure 4 (a) Relative distribution of U(VI) species as a function of pH; (b) effect of solid content on U(VI) and HA sorption to CD/GO. T = 288 K, I = 0.01 mol/L $NaClO_4$, C[U(VI) $_{(initial)}$] = 24 mg/L, C[HA$_{(initial)}$] = 10.0 mg/L, pH = 5.0 ± 0.1.

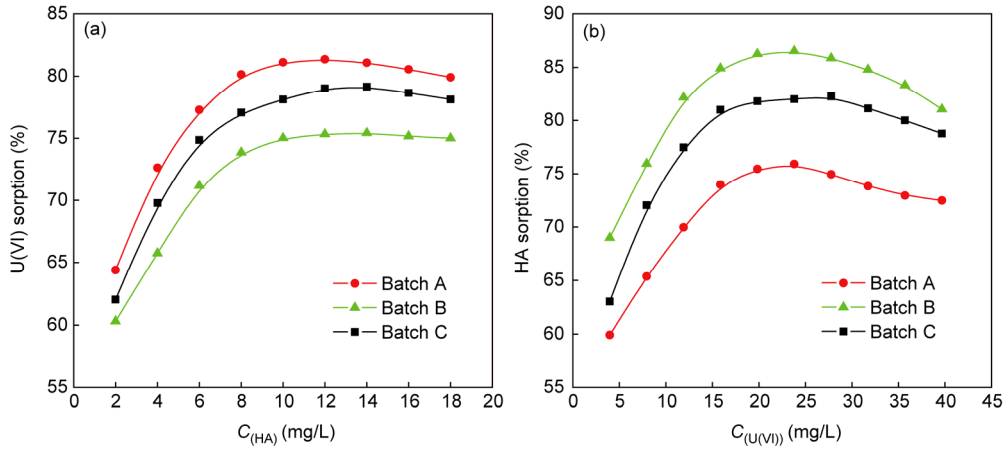

Figure 5 (a) Effect of HA concentrations on U(VI) sorption on CD/GO; (b) effect of U(VI) concentrations on HA sorption on CD/GO. T = 288 K, I = 0.01 mol/L $NaClO_4$, C[U(VI) $_{(initial)}$] =24 mg/L, C[HA$_{(initial)}$] = 10.0 mg/L, pH = 5.0 ± 0.1.

plexes with the HA, and then can be adsorbed together onto the surface of CD/GO. For the Batch B system, the HA has a different chemical composition and the range of its molecular weights is large, which results in different sorption affinities between HA and CD/GO. It has been proven that HA is composed of low molecular-weight components with

hydrophobic groups and high molecular-weight components with hydrophilic groups [32]. When HA is added to CD/GO solution, hydrophobic and low molecular-weight components are adsorbed onto CD/GO, while the hydrophilic and high molecular-weight components remain in solution. When U(VI) is subsequently added into the system and forms complexes with the free HA molecules in solution, the lowest U(VI) sorption of the three batch tests results (in the Batch B system). For the Batch C, U(VI) and HA first form complexes and are adsorbed onto the CD/GO. There may also be a part of U(VI) that is directly adsorbed onto the CD/GO. Therefore, the sorption of U(VI) in the Batch C system is higher than that of the U(VI) in the Batch B system, but lower than that of the U(VI) in the Batch A system.

U(VI) concentration (denoted as $C_{U(VI)}$) also affects HA sorption for all three batch tests (Figure 5(b)). HA sorption first rises and then maintains a high level as $C_{U(VI)}$ increases. The packing, spacing, or alignment of the adsorbed HA are gradually affected by increasing the $C_{U(VI)}$, until it achieves maximum sorption. $C_{U(VI)}$ significantly affects HA sorption; in addition, as previously noted, the mechanisms of the three batch tests are different. For the Batch B, after HA is equilibrated with CD/GO, more HA molecules are adsorbed on CD/GO than on Batch A or Batch C. On these basis of the investigations, we can conclude that the enhancement of simultaneous sorption of U(VI) and HA on CD/GO is mainly governed by electrostatic interaction and the formation of ternary cation-anion surface complexes. Our results are consistent with the work of Ren *et al.* [35], where the retention of Cu(II) was governed by the interaction of Cu-phosphate aqueous complexes with γ-Al_2O_3.

3.6 Sorption isotherms

The sorption isotherms of U(VI) and HA on CD/GO are shown in Figure 6. The experimental data are simulated by the Langmuir ($C_s = \frac{bC_{s\,max}C_e}{1+bC_e}$) and Freundlich ($C_s = K_F C_e^{\,n}$) models (where C_e is the final concentration of U(VI) or HA in solution after equilibrium (mg/g), C_s is the amount of U(VI) or HA adsorbed on CD/GO (mg/g), $C_{s\,max}$ is the maximum amount of U(VI) or HA adsorbed on CD/GO (mg/g) at complete monolayer coverage (mg/g), and b (L/mg) is a Langmuir constant that relates to the sorption heat; K_F ($mg^{1-n}L^n/g$) represents the sorption capacity when the equilibrium concentration of metal ions equals to 1, and n represents the degree of dependence of sorption with equilibrium concentration).

The relative parameters of the Langmuir and Freundlich models are shown in Table 2. From the R^2 values, we can conclude that the Langmuir model fits the U(VI) and HA sorption isotherms better than the Freundlich model (Figure 6). The maximum adsorption capacities ($C_{s\,max}$) of U(VI) are 97.3 mg/g for CD/GO in the absence of HA and 103.9 mg/g in the presence of HA. Moreover, compared to $C_{s\,max}$ values of U(VI) sorption on other sorbents such as raw MWCNTs (16.2 mg/g U(VI) at pH 5.0 and T = 298 K) [36], plasma-functionalized MWCNTs (75.1 mg/g U(VI) at pH 5.6 and T = 303 K) [28], marine-algae-and-yeast-immobilized silica gel (56.7 mg/g U(VI) at pH 4 and T = 303 K) [37], and manganese-oxide-coated zeolite (17.6 mg/g U(VI) at pH 6 and T = 293 K) [38], one can see that CD/GO has much higher sorption capacity than other sorbents. The $C_{s\,max}$ values of HA are 32.6 mg/g for CD/GO in the absence of U(VI) and 43.2 mg/g in the presence of U(VI). The above results demonstrate that the adsorption capacity of U(VI) is increased in the presence of HA, and the adsorption capacity of HA is also increased in the presence of U(VI). Accordingly, CD/GO could be a promising adsorbent for simultaneous enrichment of U(VI) and HA from aqueous solutions in practical application.

4 Conclusions

This work highlights the simultaneous sorption of U(VI)

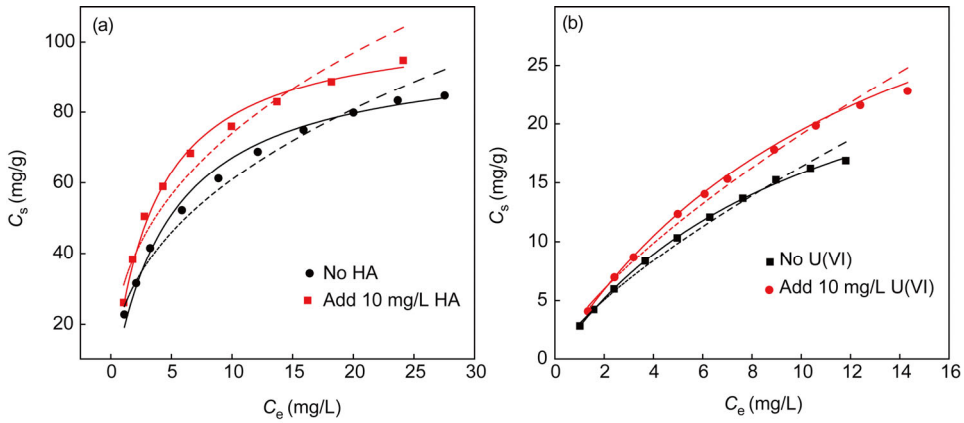

Figure 6 (a) Langmuir and Freundlich sorption isotherms of U(VI) on CD/GO in the absence of HA (marked as "no HA") and in the presence of 10 mg/L HA (marked as "add 10 mg/L HA"); (b) Langmuir and Freundlich sorption isotherms of HA on CD/GO in the absence of U(VI) (marked as "no U(VI)") and in the presence of 10 mg/L U(VI) (marked as "add 10 mg/L U(VI)"). T = 288 K, pH = 5.0 ± 0.1, m/V = 0.1 g/L, I = 0.01 mol/L $NaClO_4$.

Table 2 Parameters of the Langmuir and Freundlich isotherms

Type	Langmuir			Freundlich		
	$C_{s\,max}$ (mg/g)	b (L/mg)	R^2	k_F ($mg^{1-n}L^n/g$)	n	R^2
CD/GO-U(VI)	97.328	0.217	0.991	26.204	0.369	0.983
CD/GO-U(VI) HA	103.935	0.312	0.994	33.780	0.337	0.966
CD/GO-HA	32.579	0.094	0.998	3.454	0.663	0.991
CD/GO-HA U(VI)	43.230	0.079	0.999	4.178	0.652	0.991

and organic pollutants from aqueous solutions. The enhancement of simultaneous sorption of U(VI) and HA onto CD/GO was governed by electrostatic interaction and formation of ternary cation-anion surface complexes. The presence of HA both enhanced U(VI) sorption at low pH and reduced U(VI) sorption at high pH, whereas the presence of U(VI) enhanced HA sorption. The surface-adsorbed HA can act as a "bridge" between U(VI) and CD/GO and can form strong surface complexes with U(VI). The sorption isotherms of U(VI) and HA on CD/GO can be well simulated by the Langmuir model. The CD/GO presents promising application potential as a sorbent for the effective removal of U(VI) and organic pollutants during environmental pollution cleanup in the near future, when large-scale synthesis of GO can be economically undertaken.

This work was supported by the National Natural Science Foundation of China (91326202, 21375148, 21207136, 21225730) and the Hefei Center for Physical Science and Technology (2012FXZY005).

1 Zhu Y, Murali S, Cai W, Li X, Suk JW, Potts JR, Ruoff RS. Graphene and graphene oxide: synthesis, properties, and applications. *Adv Mater*, 2010, 22: 3906–3924
2 Wang Q, Wang XK, Chai ZF, Hu WP. Low-temperature plasma synthesis of carbon nanotubes and graphene based materials and their fuel cell applications. *Chem Soc Rev,* 2013, 42: 8821–8834
3 Zhao GX, Li JX, Ren XM, Chen CL, Wang XK. Few-layered graphene oxide nanosheets as superior sorbents for heavy metal ion pollution management. *Environ Sci Technol*, 2011, 45: 10454–10462
4 Zhao GX, Jiang L, He YD, Li JX, Dong HK, Wang XK, Hu WP. Sulfonated graphene for persistent aromatic pollutant management. *Adv Mater*, 2011, 23: 3959–3963
5 Zhao GX, Wen T, Yang XT, Yang SB, Wang XK. Preconcentration of U(VI) ions on few-layered graphene oxide nanosheets from aqueous solutions. *Dalton Trans*, 2012, 41: 6182–6188
6 Dreyer DR, Park S, Bielawski CW, Ruoff RS. The chemistry of graphene oxide. *Chem Soc Rev*, 2010, 39: 228–240
7 Park S, Lee KS, Bozoklu G, Cai W, Nguyen ST, Ruoff RS. Graphene oxide papers modified by divalent ions-enhancing mechanical properties via chemical cross-linking. *ACS Nano*, 2008, 2: 572–578
8 Xu YX, Wu Q, Sun YQ, Bai H, Shi GQ. Three-dimensional self-assembly of graphene oxide and DNA into multifunctional hydrogels. *ACS Nano*, 2010, 4: 7358–7362
9 Xiang DS, Zhang AH, Luo M, Ji XH, He ZK. Graphene oxide and molecular beacons-based multiplexed DNA detection by synchronous fluorescence analysis. *Sci China Chem*, 2013, 56: 380–386
10 Sun YB, Shao DD, Chen CL, Yang SB, Wang XK. Highly efficient enrichment of radionuclides on graphene oxide supported polyaniline. *Environ Sci Technol*, 2013, 47: 9904–9910
11 Chen Y, Chen L, Bai H, Li L. Graphene oxide-chitosan composite hydrogels as broad-spectrum adsorbents for water purification. *J Mater Chem A*, 2013, 1: 1992–2001
12 Arkas M, Allabashi R, Tsiourvas D, Mattausch EM, Perfler R. Organic/inorganic hybrid filters based on dendritic and cyclodextrin "nanosponges" for the removal of organic pollutants from water. *Environ Sci Technol*, 2006, 40: 2771–2777
13 Saenger W, Jacob J, Gessler K, Steiner T, Hoffmann D, Sanbe H, Takaha T. Structures of the common cyclodextrins and their larger analogues beyond the doughnut. *Chem Rev*, 1998, 98: 1787–1802
14 Berto S, Bruzzoniti MC, Cavalli R, Perrachon D, Prenesti E, Sarzanini C, Tumiatti W. Synthesis of new ionic β-cyclodextrin polymers and characterization of their heavy metals retention. *J Incl Phenom Macrocycl Chem*, 2007, 57: 631–636
15 Galia A, Navarre EC, Scialdone O, Ferreira M, Filardo G, Tilloy S, Monflier E. Complexation of phosphine ligands with peracetylated β-cyclodextrin in supercritical carbon dioxide: spectroscopic determination of equilibrium constants. *J Phy Chem B*, 2007, 111: 2573–2578
16 Navaza A, Iroulart MG, Navaza J. A monomeric uranyl hydroxide system obtained by inclusion in the β-cyclodextrin cavity. *J Coord Chem*, 2000, 51: 153–168
17 Gorman-Lewis D, Elias PE, Fein JB. Sorption of aqueous uranyl complexes onto Bacillus subtilis cells. *Environ Sci Technol*, 2005, 39 : 4906–4912
18 Wang XL, Yuan LY, Wang YF, Li ZJ, Lan JH, Liu YL, Feng YX, Zhao YL, Chai ZF, Shi WQ. Mesoporous silica SBA-15 functionalized with phosphonate and amino groups for uranium uptake. *Sci China Chem*, 2012, 55: 1705–1711
19 Anke M, Seeber O, Müller R, Schäfer U, Zerull J. Uranium transfer in the food chain from soil to plants, animals and man. *Chem Erde-Geochem*, 2009, 69: 75–90
20 Yang SB, Hu J, Chen CL, Shao DD, Wang XK. Mutual effects of Pb(II) and humic acid sorption on multiwalled carbon nanotubes/polyacrylamide composites from aqueous solutions. *Environ Sci Technol*, 2011, 45: 3621–3627
21 Zhang X, Bai R. Mechanisms and kinetics of humic acid sorption onto chitosan-coated granules. *J Colloid Interf Sci*, 2003, 264: 30–38
22 Hirata M, Gotou T, Horiuchi S, Fujiwara M, Ohba M. Thin-film particles of graphite oxide 1: High-yield synthesis and flexibility of the particles. *Carbon*, 2004, 42: 2929–2937
23 Li J, Zhang SW, Chen CL, Zhao GX, Yang X, Li JX, Wang XK. Removal of Cu(II) and fulvic acid by graphene oxide nanosheets decorated with Fe_3O_4 nanoparticles. *ACS Appl Mater Interf*, 2012, 4: 4991–5000
24 Guo YJ, Guo SJ, Li J, Wang EK, Dong SJ. Cyclodextrin-graphene hybrid nanosheets as enhanced sensing platform for ultrasensitive determination of carbendazim. *Talanta*, 2011, 84: 60–64
25 Yang ST, Zong PF, Sheng GD, Wang Q, Wang XK. Fabrication of β-cyclodextrin conjugated magnetic HNT/iron oxide composite for high-efficient decontamination of U (VI). *Chem Eng J*, 2012, 214: 376–385
26 Shao DD, Sheng GD, Chen CL, Wang XK, Nagatsu M. Removal of polychlorinated biphenyls from aqueous solutions using β-cyclodextrin grafted multiwalled carbon nanotubes. *Chemosphere*, 2010, 79: 679–685
27 Ding DX, Liu XT, Hu N, Li GY, Wang YD. Removal and recovery of uranium from aqueous solution by tea waste. *J Radioanal Nucl Chem*, 2012, 293: 735–741
28 Song MM, Wang Q, Meng YD. Removal of UO_2^{2+} from aqueous solution by plasma functionalized MWCNTs. *J Radioanal Nucl Chem*, 2012, 293: 899–906
29 Yan WL, Bai R. Sorption of lead and humic acid on chitosan hydrogel beads. *Water Res*, 2005, 39: 688–698
30 Floroiu RM, Davis AP, Torrents A. Cadmium sorption on aluminum oxide in the presence of polyacrylic acid. *Environ Sci Technol*, 2001, 35: 348–353
31 Myneni SCB, Brown JT, Martinez GA, Meyer-Ilse W. Imaging of humic substance macromolecular structures in water and soils. *Science*, 1999, 286: 1335–1337

32 Chen CL, Wang XK, Jiang H, Hu WP. Direct observation of macromolecular structures of humic acid by AFM and SEM. *Colloid Surf A*, 2007, 302: 121–125
33 Collins CR, Ragnarsdottir KV, Sherman DM, Effect of inorganic and organic ligands on the mechanism of cadmium sorption to goethite. Geochim. *Cosmochim Acta*, 1999, 63: 2989–3002
34 Evans N, Warwick P, Lewis T, Bryan N. Influence of humic acid on the sorption of uranium (IV) to kaolin. *Environ Chem Lett*, 2011, 9: 25–30
35 Ren XM, Yang ST, Tan XL, Chen CL, Sheng GD, Wang XK. Mutual effects of copper and phosphate on their interaction with γ-Al_2O_3: combined batch macroscopic experiments with DFT calculations. *J Hazard Mater*, 2012, 237–238: 199–208
36 Shao DD, Jiang ZQ, Wang XK, Li JX, Meng YD. Plasma induced grafting carboxymethyl cellulose on multiwalled carbon nanotubes for the removal of UO_2^{2+} from aqueous solution. *J Phys Chem B*, 2009, 113: 860–864
37 Aytas S, Turkozu DA, Gok C. Biosorption of uranium(VI) by bifunctionalized low cost biocomposite adsorbent. *Desalination*, 2011, 280: 354–362
38 Han R, Zou W, Wang Y, Zhu L. Removal of uranium (VI) from aqueous solutions by manganese oxide coated zeolite: discussion of sorption isotherms and pH effect. *J Environ Radioact*, 2007, 93: 127–143